


Hyperfine interactions in nanocrystallized NANOPERM-type metallic glass containing Mo

M. Cesnek¹  · D. Kubániová² · J. Kohout² ·
P. Křišťan² · H. Štěpánková² · K. Závěta² ·
A. Lančok³ · M. Štefánik¹ · M. Miglierini¹

Published online: 27 September 2016
© Springer International Publishing Switzerland 2016

Abstract NANOPERM-type alloy with chemical composition $\text{Fe}_{76}\text{Mo}_8\text{CuB}_{15}$ was studied by combination of ^{57}Fe Mössbauer spectroscopy and $^{57}\text{Fe}(^{10}\text{B},^{11}\text{B})$ nuclear magnetic resonance in order to determine distribution of hyperfine magnetic fields and evolution of relative concentration of Fe-containing crystalline phases within the surface layer and the volume of the nanocrystallized ribbons with annealing temperature. Differential scanning calorimetry revealed two crystallization stages at $T_{x1} \sim 510$ °C and $T_{x2} \sim 640$ °C, connected to precipitation of α -Fe and Fe(Mo,B) nanocrystals, respectively. The amorphous and partially crystalline state was obtained by annealing at several temperatures in the range 510–650 °C. The combination of conversion electron (CEMS) and transmission Mössbauer spectrometry (TMS) showed that annealing induces crystallization starting from both surfaces of the ribbons. For the as-quenched sample, scanning electron microscopy (SEM) and CEMS revealed significant differences in the “air” and “wheel” sides of the ribbons, crystallites were preferentially formed at the latter. While SEM micrographs of annealed samples showed various mean diameters of the crystals at opposite sides of the ribbons, the amounts of crystalline volume derived from the CEMS spectra approximately equaled. Mössbauer spectra of annealed samples contained narrow sextet ascribed to crystalline α -Fe phase, three sextets with distribution of hyperfine field assigned to the interface regions

This article is part of the Topical Collection on *Proceedings of the International Conference on Hyperfine Interactions and their Applications (HYPERFINE 2016), Leuven, Belgium, 3–8 July 2016*

✉ M. Cesnek
martin.cesnek@jfifi.cvut.cz

¹ Department of Nuclear Reactors, Faculty of Nuclear Science and Physical Engineering, Czech Technical University in Prague, V Holešovičkách 2, 180 00 Prague, Czech Republic

² Department of Low Temperature Physics, Faculty of Mathematics and Physics, Charles University, V Holešovičkách 2, 180 00 Prague, Czech Republic

³ Institute of Inorganic Chemistry AS CR, v. v. i., Husinec-Řež 1001, 250 68 Řež, Czech Republic

of the nanocrystals and the contribution of the amorphous phases. In-field TMS performed at 4.2 K with magnetic moments aligned by external magnetic field enabled to properly determine in particular the contribution of the amorphous phases in the samples. Resulting distributions of the hyperfine fields were compared with $^{57}\text{Fe}(^{10}\text{B},^{11}\text{B})$ nuclear magnetic resonance (NMR) spectra.

Keywords Mössbauer spectrometry · Nuclear magnetic resonance · Metallic glass · Hyperfine interactions

1 Introduction

Metallic amorphous glasses (MG), also denoted as metallic amorphous alloys, exhibit unique soft magnetic properties as low coercivity, high permeability and relatively high magnetic saturation [1, 2], caused mostly by the lack of long range atomic order in this multicomponent system [3]. By controlling their chemical composition, it is possible to tailor their physical properties. Together with low production costs, it provides the basis for promising applications in the field of power engineering - e.g. in transformers, electric motors, sensors etc. [4]. In comparison with polycrystalline materials, MGs exhibit lower eddy current losses due to their high electrical resistivity and low thickness [5].

The physical properties of nanocrystalline alloys (NC) prepared by controlled crystallization of MGs with appropriate composition can be further modified by varying the size of crystalline grains, their morphology and structural arrangement [6].

Particular type of Fe-based MGs, NANOPERM-type alloys with composition Fe-X-B or Fe-X-B-Cu, exhibits relatively high values of magnetic permeability and relatively low Curie temperature in the range 300–400 K [7]. In the following text, we present a study of $\text{Fe}_{76}\text{Mo}_8\text{Cu}_1\text{B}_{15}$ MG that displays good soft magnetic properties [8]. This alloy was designed as a model system for Mössbauer spectrometry studies aimed at better understanding of its structural features [9, 10].

In our study, we employed both transmission Mössbauer spectrometry (TMS), providing the information on the hyperfine interactions in the bulk of the sample, and conversion electron Mössbauer spectrometry (CEMS) which scans the immediate surface to the depth of approximately 200 nm, respectively. Together with ^{57}Fe nuclear magnetic resonance measurement (NMR), which was demonstrated in [11] to be able to distinguish the structural features of similar isotopically enriched Fe-based MG and NC alloys, these three approaches provided comprehensive information on how the annealing affects the hyperfine interactions with special attention to the hyperfine magnetic fields and their distributions. Samples of $\text{Fe}_{76}\text{Mo}_8\text{Cu}_1\text{B}_{15}$ metallic glasses were investigated in their as-quenched state and after annealing at 510, 530, 550, and 650 °C in a vacuum for 1 hour to cover the whole crystallization process.

2 Experimental

2.1 Samples

The amorphous NANOPERM-type alloy with a nominal chemical composition $\text{Fe}_{76}\text{Mo}_8\text{Cu}_1\text{B}_{15}$ was prepared by a single-roller planar flow casting without any protective atmosphere in the form of about 20 μm thick ribbons. Rapid cooling of the samples

during the process prohibits its crystallization, thus ensuring the preparation of fully amorphous material. Chemical composition was checked by optical emission spectrometry with inductively coupled plasma (Mo, B) and flame atomic absorption spectrometry (Fe, Cu).

2.2 Scanning electron microscopy

The surface structure of the samples was observed using a Tescan FERA 3 tool with 5 kV accelerating voltage.

2.3 Mössbauer spectrometry

All MS experiments were accomplished with a conventional constant acceleration spectrometer by Wissel equipped with a ^{57}Co source in Rh matrix. The spectrometer was calibrated using a standard 12.5 μm foil of $\alpha\text{-Fe}$ at room temperature. Low-temperature TMS experiments at liquid helium temperature were performed in an SVT-400 bath cryostat by Janis. The in-field spectra were acquired at 4.2 K in magnetic field of 6 T oriented parallel with the plane of the absorber and thus perpendicularly to the direction of γ beam. The relatively high external field may be needed if the crystallization produces some magnetically hard products. CEMS spectra were measured only at room temperature. Spectral parameters were derived by the help of the CONFIT[®] [12] fitting software. This fitting programme makes it possible to employ only Gauss-like distribution of hyperfine parameters. The more complicated distributions are then modelled by introducing additional Gaussian distribution(s).

2.4 ^{57}Fe nuclear magnetic resonance

^{57}Fe NMR spectra were measured by the spin echo Car-Purcell-Meiboom-Gill (CPMG) sequence using a phase coherent pulse spectrometer Bruker Avance with averaging technique and Fourier transform of the time domain signal. All measurements were performed in zero magnetic field at 4.2 K. The frequency-swept spectra were recorded using a frequency step of 0.2 MHz, the NMR probe was properly tuned and matched at each excitation frequency. The length of the first radiofrequency (RF) pulse in the CPMG sequence was 1.5 μs . When the optimal amplitude of the applied RF pulse varied significantly within the spectral range, the particular spectra were successively measured for the specific excitation conditions and the final spectral profile was constructed as an envelope of the particular spectral shapes.

3 Results and discussion

3.1 Scanning electron microscopy

Crystallites are formed at both sides of the ribbon during the preparation. Micrographs shown in Fig. 1 point out the fact that the crystals growing at $T_A = 510\text{ }^\circ\text{C}$ at the “wheel” side are larger than ones observed at the “air” side, indicating higher concentration of the nuclei at the latter. Under further increased annealing temperature to 650 $^\circ\text{C}$, new crystallites are able to form and crystal growth proceed. However, as will be shown later, the relative volume of the crystalline phases is practically identical as given by CEMS.

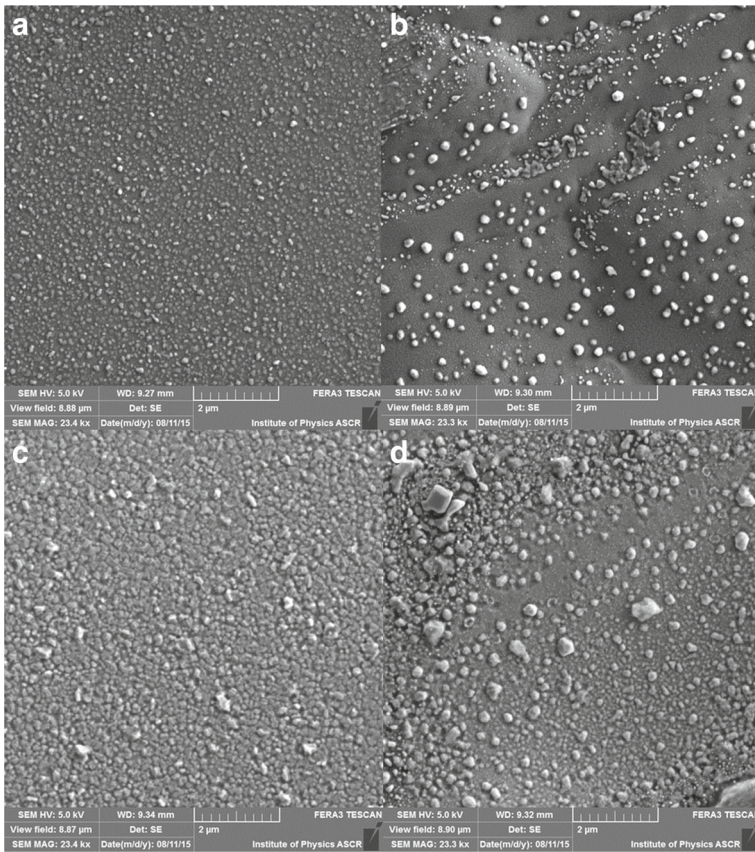


Fig. 1 SEM images of “air” and “wheel” sides of the nanocrystalline ribbon taken after the 1st crystallization ($T_A = 510\text{ }^\circ\text{C}$) - “air” side shown in (a) and “wheel” side in (b), and after the 2nd crystallization ($T_A = 650\text{ }^\circ\text{C}$) - “air” side (c) and “wheel” side (d)

3.2 Mössbauer spectrometry

In this particular case, low temperature (4.2 K) Mössbauer spectroscopy provides better resolution due to dominating dipole magnetic interactions. For acquisition of the in-field Mössbauer spectra (shown in Fig. 2), the external field of 6 T was applied in the sample plane, thus aligning magnetic moments along its direction.

Distributions of hyperfine magnetic field determined from the spectra are characterized by the corresponding $P(B)$ distribution plotted in Fig. 3. Because of the antiparallel orientation of Fe magnetic moment and hyperfine field a shift of $P(B)$ towards lower fields is observed. The distribution of the hyperfine fields in the in-field spectra is narrower in particular for the contribution from the amorphous phases, allowing to better distinguish their contribution to spectral intensity. During the fitting of all in-field spectra, the relative line intensities were fixed to 3:4:1 and relative ratio of α -Fe contribution to other magnetically ordered phases in both low temperature measurements was kept the same.

In the case of the as-quenched sample, the spectra were fitted by two Gauss-like distributed sextets which correspond to the amorphous matrix. For additionally annealed

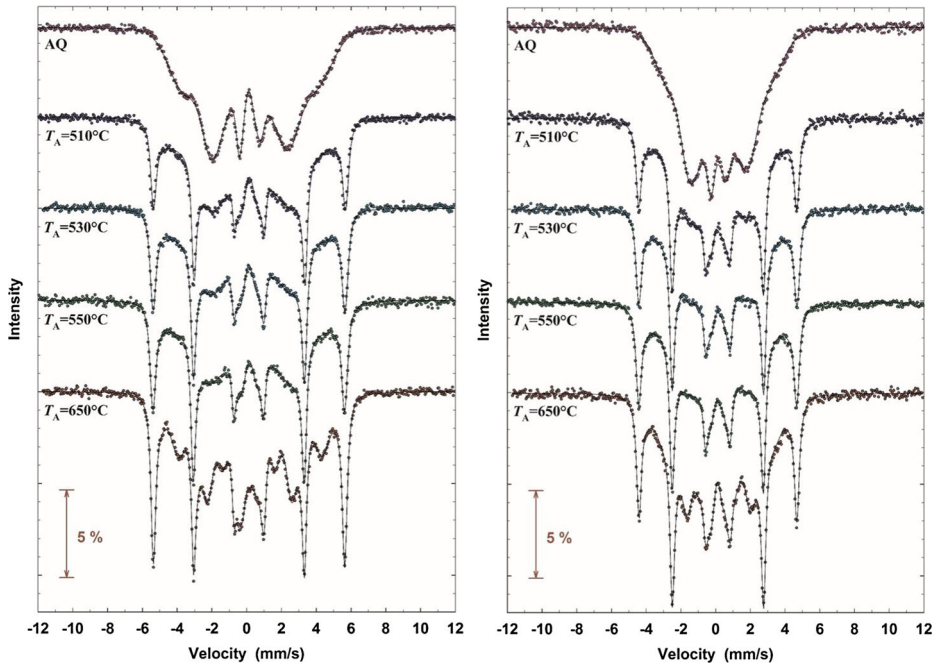


Fig. 2 ^{57}Fe transmission Mössbauer spectra at various annealing temperatures of the as-quenched (AQ) and nanocrystalline $\text{Fe}_{76}\text{Mo}_8\text{Cu}_1\text{B}_{15}$ alloy taken at liquid helium temperature without any external magnetic field (*left*) and in external magnetic field of 6 T (*right*) oriented perpendicularly to the γ beam

samples up to 550 °C, the spectra reveal major sextet clearly belonging to α -Fe and a minor one of a magnetically ordered phase which, based on its hyperfine parameters $IS \sim 0.19$ mm/s, $QS \sim -0.012$ mm/s and $B_{\text{hf}} \sim 32.5$ T, can be the interfacial phase between α -Fe and the residual matrix or possibly bcc-Fe with one Mo atom in its first coordination shell [13, 14]. Both contributions were fitted by distributions of hyperfine magnetic fields. The relative intensities of the 2nd and 5th lines in the sextets were left as free fitted parameters, yielding thus information about the average orientation of magnetization for the given phase.

The contribution of the residual amorphous matrix to the spectra was fitted by two to three distributed sextets and one doublet with distribution of quadrupole splitting representing non-magnetic contribution. In addition, the amount of the α -Fe nanocrystalline phase at 4.2 K is slightly but regularly higher compared to the room temperature measurement which indicates a higher number of “blocked” vs superparamagnetic particles at low temperatures.

During second crystallization ($T = 650$ °C), new neighbourhoods of Fe in magnetically ordered phases are formed. Besides the contributions of α -Fe and a minor phase, the Mössbauer spectra contain three distributed sextets. Observed hyperfine parameters suggest that these components are due to Fe with nearest neighbourhood similar to crystalline Fe_3B ($IS \sim 0.193$ mm/s, $QS \sim 0.02$ mm/s, $B_{\text{hf}} \sim 25.8$ T) [15, 16], B containing magnetic phase ($IS \sim 0.134$ mm/s, $QS \sim -0.07$ mm/s, $B_{\text{hf}} \sim 16.6$ T) and Mo(Cu) containing magnetic phase ($IS \sim 0.073$ mm/s, $QS \sim 0.04$ mm/s, $B_{\text{hf}} \sim 8.7$ T) [17]. For the sample annealed at 650 °C, the spectra taken without the external field indicate that the magnetization has a considerable out-of-plane component [18]. This is in contrast to the samples annealed at lower

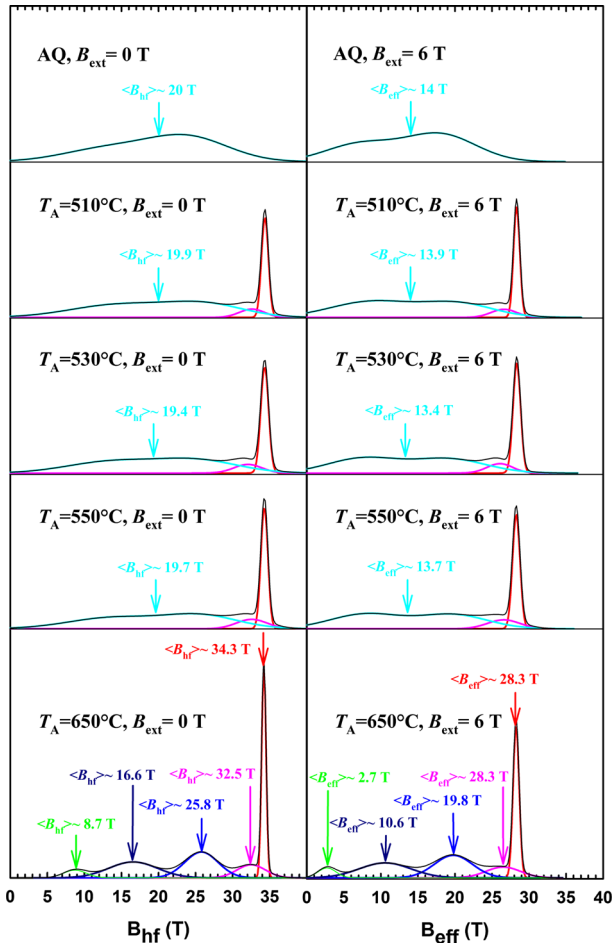


Fig. 3 Distributions of hyperfine magnetic fields $P(B)$ at various annealing temperatures derived from ^{57}Fe transmission Mössbauer spectra acquired at 4.2 K without any external magnetic field (a) and in external magnetic field of 6 T (b) oriented perpendicularly to the γ beam. Color code – α -Fe (red), interfacial phase or bcc Fe with one Mo as n.n. (pink), Fe_3B -like neighbourhoods (light blue), B containing magnetically ordered neighbourhoods (dark blue), Mo containing magnetically ordered neighbourhoods (green), amorphous component (cyan), sum of all fitted components (black)

temperatures, where the spectra correspond to the orientation of magnetization essentially in the ribbon plane.

CEMS spectra at room temperature (Fig. 4) were acquired from both sides of the ribbons. By comparison with room temperature TMS (given in Fig. 5), providing integrated information over the whole volume of the sample, we could observe the differences in the crystallization of α -Fe between the surface layers and the ribbon volume. As shown in Fig. 6, crystallization starts from both sides of the ribbon [19] with slightly higher volume of the crystalline phase at the “air” side. Even in the as-quenched state, the air side contains some crystalline seeds due to lower rate of cooling with respect to the wheel side as already observed with similar compositions of the ribbons in [20]. After second crystallization

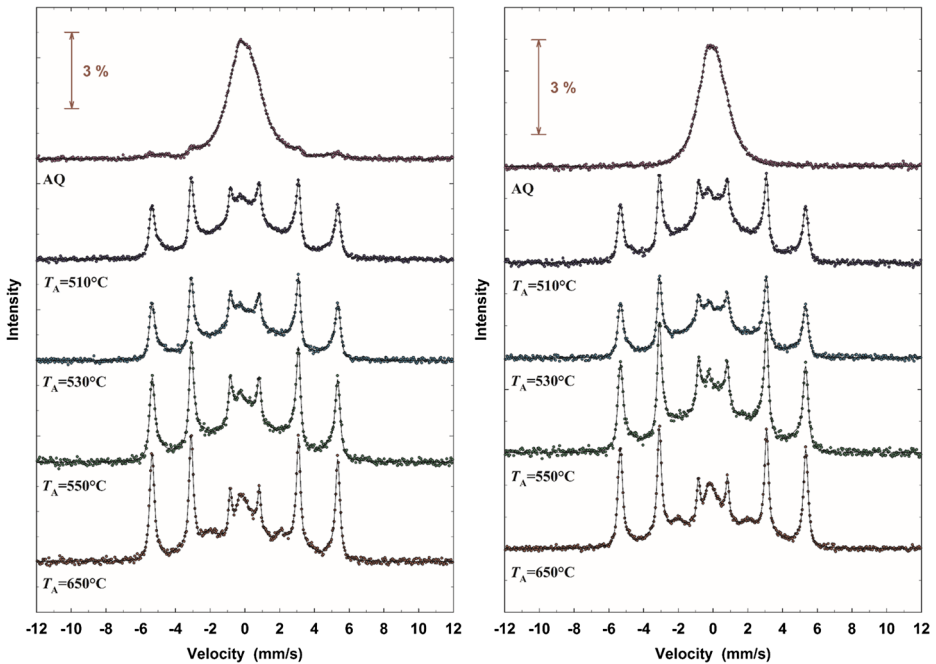


Fig. 4 ^{57}Fe conversion electron Mössbauer spectra for various annealing temperatures taken at room temperature from the “air” side of the ribbons (*left*) and “wheel” side of the ribbons (*right*)

($T = 650\text{ }^\circ\text{C}$), the relative content of the crystalline $\alpha\text{-Fe}$ determined from room and low temperature transmission Mössbauer spectra comes to equal within the experimental error, indicating disappearance of superparamagnetic nanograins.

3.3 ^{57}Fe nuclear magnetic resonance

The results of ^{57}Fe NMR measurements are plotted in Fig. 7. In the NMR spectrum of the as-quenched sample (AQ) a broad spectral line assigned to the amorphous structure is seen. The NMR signal cannot be assigned simply to ^{57}Fe nuclei because the presence of ^{11}B (^{10}B) affects the shape of the NMR lines to a considerable degree. The NMR spectra of all annealed samples show, besides the broad line belonging to the amorphous matrix, a narrow asymmetrical line at around 46.9 MHz. In accordance with [16, 21] this line is assigned to the resonance of ^{57}Fe in $\alpha\text{-Fe}$ crystalline phase formed during the annealing process. The resonance frequency of ^{57}Fe nuclei located in $\alpha\text{-Fe}$ and having one Mo atom in its nearest coordination shell is known to be located at ~ 43 MHz but this contribution is expected to be weak and seems to be hidden in the broad spectral shapes of another origin.

In the NMR spectrum of the sample annealed at $650\text{ }^\circ\text{C}$, also formation of other crystalline phase/phases is observed. The emerging spectral shape occupies a spectral width of ~ 10 MHz and its maximum is centered at ~ 38 MHz. The optimal amplitude of RF pulse is different from that of $\alpha\text{-Fe}$ as is illustrated in Fig. 8, and moreover the signal in the frequency region 33–42 MHz exhibits faster spin-spin relaxation than the signal of $\alpha\text{-Fe}$ (see Fig. 9). This spectral region corresponds to the resonances of ^{57}Fe in tetrahedral and

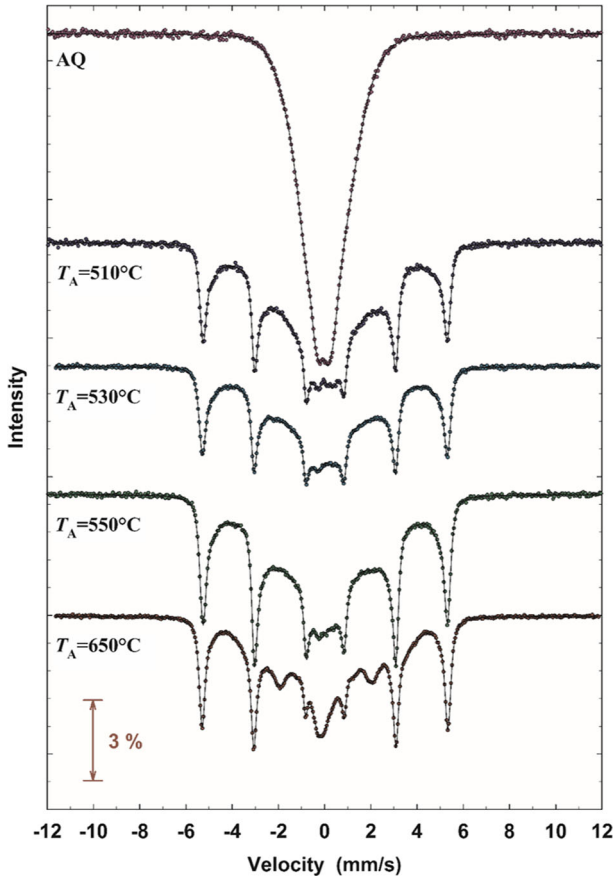


Fig. 5 ^{57}Fe transmission Mössbauer spectra for various annealing temperatures taken at room temperature

orthorhombic Fe_3B (corresponding frequencies are highlighted in Fig. 7) but crystallization of other phases, e.g. FeMo_2B_2 reported in [17, 22] is not excluded.

3.4 Hyperfine (effective) magnetic fields

The distribution of hyperfine magnetic field $P(B)$ can be obtained using both methods - Mössbauer spectrometry and ^{57}Fe NMR, respectively. Since they use the same ^{57}Fe nuclei as probe atoms in the material, in principle it is possible to compare the respective results. In order to do so, the NMR signals were first transformed from the frequency range into hyperfine field values B using γ factor 1.38156 MHz/T [23], followed by the linear frequency correction and intensity normalization according the high B -tails of the $P(B)$ distributions.

The NMR signal shape in frequency domain of about 25–45 MHz (18.1–32.6 T) is strongly affected by the contribution arising from ^{11}B (^{10}B) present in the samples [16, 21]. The observed deviations of $P(B)$ distributions towards higher B -values determined by NMR compared to those derived from MS spectra might be due to the presence of possible impurities (Mo, B) in the bcc nanocrystals.

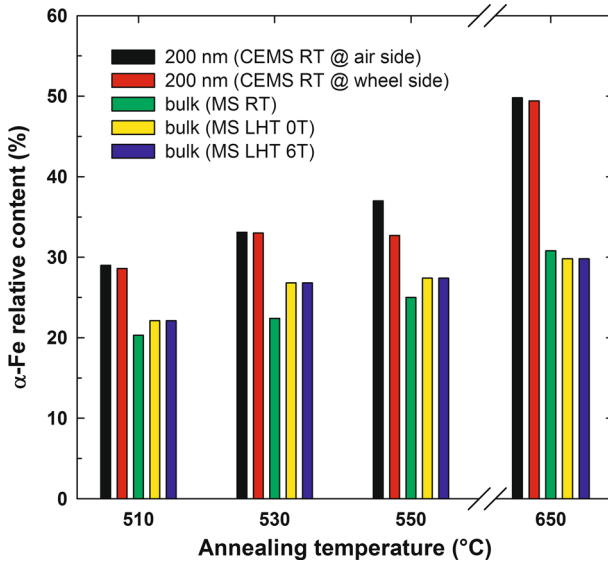


Fig. 6 Progress of the crystallization of the α -Fe phase with annealing temperature

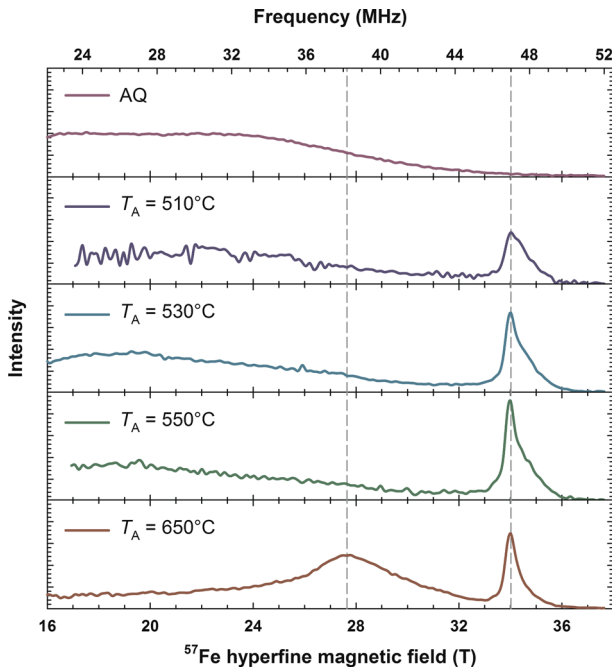


Fig. 7 The NMR spectra measured in the as-quenched sample of $Fe_{76}Mo_8Cu_{15}B_{15}$ and after annealing. The plotted spectra were evaluated from the first two echoes in the CPMG echo train. The spectra were recorded at 4.2 K in zero external magnetic field

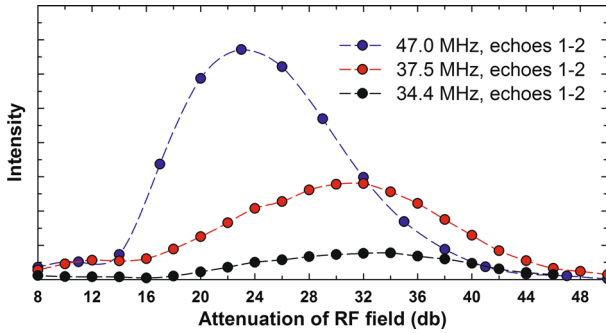


Fig. 8 Dependences of NMR signal intensities on the amplitude of the applied RF field at various frequencies

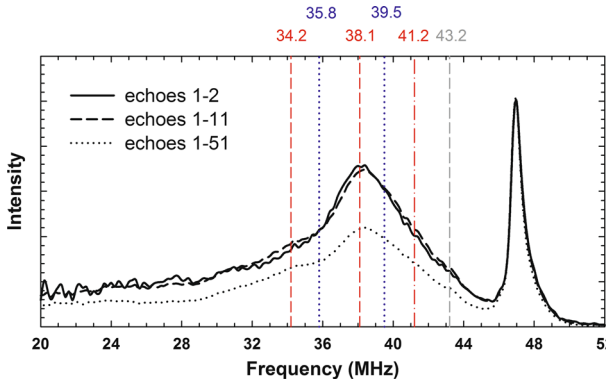


Fig. 9 The NMR spectral shapes of the sample annealed at 650 °C evaluated from various echoes and normalized to the maximum of the intensity. Red, blue and gray lines denote resonant frequencies of tetrahedral Fe₃B, orthorhombic Fe₃B and satellite of α -Fe spectral line, according to [16]

4 Conclusions

Here we presented the study on the samples of NANOPERM-type alloy with composition Fe₇₆Mo₈Cu₁B₁₅ prepared by a single-roller planar flow casting. By combination of high-resolution nuclear techniques – Mössbauer spectrometry and ⁵⁷Fe nuclear magnetic resonance – which use ⁵⁷Fe nuclei as a local probe, we investigated the hyperfine interactions in the ribbons annealed at temperatures 510-650 °C. We determined the relative content of the magnetically ordered Fe-based phases formed during the thermal treatment, the effect of annealing on the distribution of hyperfine magnetic fields and shed light on the crystallization progress on both surfaces and over the ribbon volume.

Within the first crystallization peak (480-550 °C), two magnetically ordered products containing Fe were observed: one was identified as nanograins of bcc Fe and the other was ascribed to an interfacial phase on their surface. The latter one is, however, hardly distinguishable from the possible contribution of Fe in bcc lattice with 1 Mo atom as the nearest neighbor. When the ribbons were annealed at the range of the second crystallization, new magnetically ordered phases with Fe additionally appeared which according to their

Mössbauer parameters and behaviour at NMR probably corresponded to Fe_3B and more complicated Fe phases containing Mo(Cu) and B.

The combination of conversion electron and transmission Mössbauer spectrometry with various information depths confirmed that annealing induces crystallization starting from both surfaces of the ribbon. During the crystallization, higher relative volume of crystallites was found in the surface layers compared to the inner volume of the ribbon.

Acknowledgments Financial support by the research grant GAČR 14-12449S is gratefully acknowledged.

References

- Inoue, A.: Stabilization of metallic supercooled liquid and bulk amorphous alloys. *Acta Mater.* **48**, 279–306 (2000)
- Kong, F.L., Chang, C.T., Inoue, A., Shalaa, E., Al-Marzouki, F.: Fe-based amorphous soft magnetic alloys with high saturation magnetization and good bending ductility. *J. Alloys Compd.* **615**, 163–166 (2014)
- Yu, Q., Wang, X.D., Lou, H.B., Cao, Q.P., Jiang, J.Z.: Atomic packing in Fe-based metallic glasses. *Acta Mater.* **102**, 116–124 (2016)
- Herzer, G.: Modern soft magnets: Amorphous and nanocrystalline materials. *Acta Mater.* **61**, 718–734 (2013)
- Herzer, G., Hilzinger, H.R.: Recent developments in soft magnetic materials. *Phys. Scr.* **T24**, 22–28 (1988)
- Conde, C.F., Conde, A.: Microstructure and magnetic properties of Mo containing NANOPERM-type alloys. *Rev. Adv. Mater. Sci.* **18**, 565–571 (2008)
- Kwapuliński, P., Chrobak, A., Haneczok, G., Stokłosa, Z., Rasek, J., Lelatko, J.: Optimization of soft magnetic properties in nanoperm type alloys. *Mater. Sci. Eng. C* **23**, 71–75 (2003)
- Hasiak, M., Miglierini, M.: Effect of low temperature annealing upon magnetic properties of FeMoCuB metallic glass. *IEEE Trans. Magn.* **51**, 2000804 (2015)
- Miglierini, M., Kaňuch, T., Švec, P., Krenický, T., Vůjtek, M., Zbořil, R.: Magnetic microstructure of NANOPERM-type nanocrystalline alloys. *Phys. Status Solidi B* **243**, 57–64 (2006)
- Miglierini, M., Degmová, J., Kaňuch, T., Grenèche, J.-M.: Temperature dependence of magnetic microstructure in $\text{Fe}_{76}\text{Mo}_8\text{Cu}_1\text{B}_{15}$ nanocrystalline alloy. *Phys. Status Solidi A* **201**, 3280–3284 (2004)
- Miglierini, M., Lančok, A., Kohout, J.: Hyperfine fields in nanocrystalline Fe–Zr–B probed by ^{57}Fe nuclear magnetic resonance spectroscopy. *Appl. Phys. Lett.* **96**, 211902 (2010)
- Žák, T., Jirásková, Y.: CONFIT: Mössbauer spectra fitting program. *Surf. Interf. Anal.* **38**, 710–714 (2006)
- Marcus, H.L., Schwartz, L.H.: Mössbauer spectra of FeMo alloys. *Phys. Rev.* **162**, 259–262 (1967)
- Błachowski, A., Ruebenbauer, K., Zukrowski, J., Przewoźnik, J.: Spin and charge density on iron nuclei in the BCC Fe–Mo alloys studied by ^{57}Fe Mössbauer spectroscopy. *J. Al. Com.* **482**, 23–27 (2009)
- Abd-Elmeguid, M.M., Micklitz, H., Vincze, I.: High-pressure Mössbauer studies of amorphous and crystalline Fe_3B and $(\text{Fe}_{0.25}\text{Ni}_{0.75})_3\text{B}$. *Pys. Rev. B* **25**, 1–7 (1982)
- Pokatilov, V.S.: ^{57}Fe NMR study of amorphous and rapidly quenched crystalline Fe–B alloys. *Phys. Solid State* **51**, 143–149 (2009)
- Paluga, M., Švec, P., Janičkovič, D., Müller, D., Mrafko, P., Miglierini, M.: Nanocrystallization in rapidly quenched Fe–Mo–Cu–B: Surface and volume effects. *Rev. Adv. Mater. Sci.* **18**, 481–493 (2008)
- Kuzmann, E., Stichleitner, S., Sápi, A., Klencsár, Z., Oshtrakh, M.I., Semionkin, V.A., Kubuki, S., Homonnay, Z., Varga, L.K.: Mössbauer study of FINEMET with different permeability. *Hyperfine Interact.* **219**, 63–67 (2013)
- Miglierini, M.B., Hatala, T., Frydrych, J., Šafařová, K.: Surface crystallization of Co-containing NANOPERM-type alloys. *Hyperfine Interact.* **205**, 125–128 (2012)
- Miglierini, M., Kaňuch, T., Pavúk, M., Jiraskova, Y., Zbořil, R., Mašláň, M., Švec, P.: Evolution of structural changes in nanocrystalline alloys with temperature. *Phys. Metals Metallogr.* **104**, 335–345 (2007)
- Kohout, J., Křišťan, P., Kubániová, D., Kmječ, T., Závěta, K., Štěpánková, H., Lančok, A., Sklenka, L., Matuš, P., Miglierini, M.B.: Low temperature behavior of hyperfine fields in amorphous and nanocrystalline FeMoCuB. *J. Appl. Phys.* **117**, 17B718 (2015)

22. Pavuk, M., Miglierini, M., Vujtek, M., Mashlan, M., Zboril, R., Jiraskova, Y.: AFM and Mössbauer spectrometry investigation of the nanocrystallization process in Fe–Mo–Cu–B rapidly quenched alloy. *J. Phys. Condens. Matter* **19**, 216219 (2007)
23. Berger, S., Braun, S.: 200 and more NMR experiments. WileyVCH, Weinheim (2004)